Scientific Report

TGFβ1-induced leucine limitation uncovered by differential ribosome codon reading

Fabricio Loayza-Puch[1,*,†] (iD), Koos Rooijers[1,†], Jelle Zijlstra[1], Behzad Moumbeini[1], Esther A Zaal[2], Joachim F Oude Vrielink[1], Rui Lopes[1], Alejandro P Ugalde[1], Celia R Berkers[2] & Reuven Agami[1,3,**] (iD)

Abstract

Cancer cells modulate their metabolic networks to support cell proliferation and a higher demand of building blocks. These changes may restrict the availability of certain amino acids for protein synthesis, which can be utilized for cancer therapy. However, little is known about the amino acid demand changes occurring during aggressive and invasive stages of cancer. Recently, we developed diricore, an approach based on ribosome profiling that can uncover amino acid limitations. Here, we applied diricore to a cellular model in which epithelial breast cells respond rapidly to TGFβ1, a cytokine essential for cancer progression and metastasis, and uncovered shortage of leucine. Further analyses indicated that TGFβ1 treatment of human breast epithelial cells reduces the expression of SLC3A2, a subunit of the leucine transporter, which diminishes leucine uptake and inhibits cell proliferation. Thus, we identified a specific amino acid limitation associated with the TGFβ1 response, a vulnerability that might be associated with aggressiveness in cancer.

Introduction

The transforming growth factor-β1 (TGFβ1) has a wide variety of biological roles including cell proliferation, differentiation, cell motility and survival [1,2]. The canonical TGFβ1 pathway initiates signalling by binding to type I and type II TGFβ receptors. Upon ligand binding the two types of serine threonine protein kinase receptors form heterotetrameric complexes, which in turn phosphorylate and activate SMAD transcription factors and, after association with SMAD4, are translocated to the nucleus to activate or repress target genes [3].

TGFβ1 is essential for cancer progression and metastasis. The role of this molecule in cancer progression might seem paradoxical since it has features of tumour suppressor as well as tumour promotor. TGF-beta is a potent growth inhibitor for most cell types, including epithelial, endothelial and hematopoietic cells. TGFβ1-induced arrest occurs during G_1 and is mediated by Smad proteins, which negatively regulate the transcription of target genes like c-myc [4]. TGFβ1 cytostatic role has also been linked to the suppression of retinoblastoma protein (Rb) phosphorylation through inhibition of Cdk2-CycE [5,6].

As tumours grow, they tend to become unresponsive to TGFβ1 cytostatic activity and overexpress TGFβ1. This creates a tumour microenvironment that promotes tumour growth and metastasis [7]. The initial in vitro evidence for the pro-tumorigenic effects of TGFβ1 consisted of the induction of a mesenchymal phenotype in epithelial tumour cells (commonly known as an epithelial-to-mesenchymal transition (EMT)) after prolonged exposure to TGFβ1. EMT is a cellular process in which polarized epithelial cells acquire mesenchymal properties that allow them to become migratory and invasive as well as more resistant to apoptosis and senescence [8–10].

Recently, the response to TGFβ1 has been linked to profound changes in cellular metabolism [11,12]. Cells undergoing EMT, a process induced by TGFβ1, express high levels of dihydropyrimidine dehydrogenase (DPYP), an enzyme that degrades pyrimidines [13]. Interestingly, DPYD is not required for cell proliferation but it is essential for EMT, suggesting the existence of a specific metabolic programme in EMT. Dong *et al* reported that SNAI, a key target of TGFβ1, is critical for silencing the expression of fructose-1,6-biphosphatase (FBP1). Loss of FBP1 in basal-like breast cancer cells results in higher glucose consumption, increased glycolytic rates and ATP production under hypoxia [14]. Furthermore, metastatic cells seem to favour oxidative phosphorylation and ATP production by using

1 Division of Biological Stress Response, The Netherlands Cancer Institute, Amsterdam, The Netherlands
2 Biomolecular Mass Spectrometry and Proteomics, Bijvoet Center for Biomolecular Research, Utrecht University, Utrecht, The Netherlands
3 Erasmus MC, Rotterdam University, Rotterdam, The Netherlands
   *Corresponding author. Tel: +31 205122048; E-mail: f.loayza@nki.nl
   **Corresponding author. Tel: +31 205122079; E-mail: r.agami@nki.nl
   †These authors contributed equally to this work

the transcription coactivator peroxisome proliferator-activated receptor gamma, PGC-1α [15]. Altogether, these findings indicate that TGFβ1-induced mesenchymal cells may acquire distinctive metabolic needs that may favour invasiveness and suppress cell growth.

(Ribo-seq) profiling is a novel approach that allows the study of changes in rate of protein translation on a truly global scale. It maps the positions of ribosomes on transcripts by nuclease footprinting, generating nuclease-protected ribosome-bound mRNA fragments (RPFs) that are converted into a DNA library suitable for deep sequencing [16]. Recently, we harnessed Ribo-seq for sensing restrictive amino acids, and developed *diricore*, a procedure for differential-ribosome-measurements-of-codon-reading [17]. We showed that Ribo-seq has the potential to uncover amino acid deficiencies, vulnerabilities that can be utilized to target key metabolic pathways for cancer treatment.

Here, we applied *diricore* to a cellular model in which epithelial cells respond rapidly to TGFβ1. We found that when breast cells undergo TGFβ1-induced EMT, ribosomes accumulate at leucine codons indicating limitation of this amino acid. This effect was linked to a reduced uptake of the amino acid due to downregulation of the SLC3A2 transporter. Moreover, we found that the reduced uptake of Leucine assists in TGFβ1-induced cellular arrest while EMT remained intact. Altogether, we show that TGFβ1 treatment of breast cells exposes a limitation in the essential amino acid leucine, a deficiency that potentially can be utilized for development of targeted therapies.

Results and Discussion

We recently developed differential ribosome codon reading (diricore) to uncover amino acid limitations in cancer [17]. This approach consists of two complementary analyses, subsequence and 5′ density. The positions 12 and 15 from the 5′-end of the RPFs correspond to the P (the site occupied by the peptidyl-tRNA) and A (the site occupied by the aminoacyl-tRNA) sites of the ribosome. Increased signal at position 15 at a particular codon indicates a limitation of the corresponding amino acid [17]. We used *diricore* to study TGFβ1-induced changes in amino acid metabolism that may restrict their availability for protein synthesis. As a representing system, we used the epithelial non-transformed MCF-10A cell line and treated it with the transforming growth factor beta 1 (TGFβ1), a cytokine that control proliferation and differentiation [18,19]. In particular, we used non-induced MCF10A-inducible RAS^V12 cells as these activated the transcriptional response relatively fast (48 h) following TGFβ1 treatment (from now on these cells are referred as MCF-10A) (Fig EV1). Interestingly, *diricore* analysis of TGFβ1-treated versus untreated MCF-10A cells resulted in significant accumulation of RPFs at leucine codons (position 15) and decreased signal in position 12 (Figs 1A–C and EV2). We strengthen our *diricore* result by statistical analysis performed on three independent replicates. This indicated the highly significant effect of TGFβ1 treatment on leucine codons (*P*-value < 0.001; Fig 1D).

Leucine is an essential amino acid that when acutely depleted can affect cell proliferation via the mTOR pathway. Recently, it was shown that leucine binds to Sestrin 2 to activate mTORC1 [20]. We have previously shown that *diricore* analysis can detect global

changes in mRNA translation by examining the initiator methionine codon at position 12. A strong decrease in protein synthesis correlated with a strong deep in signal at the initiator methionine at position 12 [17]. However, we observed no decrease in *diricore* signal at position 12 of the initiator ATG (Fig 1E), suggesting that TGFβ1 treatment did not elicit acute leucine depletion that will result in global inhibition of initiation translation. In contrast, acute depletion of amino acids, or inhibition of mTOR activity by Torin1, initiated, as expected, a strong deep in position 12 of the initiator ATG (Fig 1E). We corroborated this result by Western blotting where we observed a mild reduction in phosphorylation of two key translation initiation factors of mTOR activity, S6K and 4EBP1, in limiting concentrations of leucine, an effect that was potentiated by TGFβ1 treatment (Fig EV3A). Translational efficiency (TE) analysis also showed only a mild reduction in ribosome occupancy in the mTOR target genes (Figs 1F and EV3B), whereas Torin1 and nutrient deprivation caused marked effects (Figs 1E and EV3C and D). In line with these findings, acute leucine starvation in a breast cancer cell line showed no diricore signal, while mild depletion showed a strong signal in the two least abundant leucine codons (Fig EV4A). Thus, our data so far suggest that TGFβ1 treatment of MCF10A cells provokes leucine-codon signals in *diricore,* which may indicate mild leucine limitations for protein synthesis. Our analysis of the *diricore* signals of the initiator ATG suggests that even though leucine is a signalling molecule that is required for mTOR activation [21], the presumed leucine limitation following TGFβ1 treatment did not affect global translation initiation, explaining its detection by *diricore*.

To unravel the chain of events causing the leucine signal, we initially examined changes in gene expression, as a dramatic increase in the amount of leucine codons following TGFβ1 treatment may indicate increase in demand. However, no indication for increased leucine demand was obtained when we either inspected it by RNAseq or when a correlation was made between the fraction of leucine codons and TGFβ1-induced translation efficiency changes (Fig 2A and B). Also, changes in leucine tRNA levels (Leu-tRNA) or their amino acid charging may cause such effects. While the total levels of Leu-tRNAs did not change following TGFβ1 treatment (Fig 2C), we did observe a significant increase in the relative non-aminoacylated levels of all tested Leu-tRNAs, but not the controls aspartic acid (Asp)-tRNA and valine (Val)-tRNA, following treatment (Fig 2D). These observations correlated very well with measurements of intracellular amino acids that showed strong reduction in leucine and glycine after TGFβ1 treatment (Fig EV4B). The fact that only leucine showed strong signal in diricore in response to TGFβ1 indicates that the reduced glycine level was still not limiting for protein synthesis. As lower cellular levels of leucine potentially can trigger reduced level of Leu-tRNA charging, our results so far pinpoint to cellular limitation in leucine availability for protein synthesis following TGFβ1 treatment as the underlying mechanism of the *diricore* leucine signal.

To substantiate our results and further investigate possible molecular mechanisms leading to TGFβ1-induced limitation in leucine, we examined the expression levels of genes related to leucine cellular uptake, synthesis and tRNA aminoacylation. Figure 2E shows that while TGFβ1 induced no change in the level of LARS, the only cytosolic Leu-tRNA synthetase, the level of SLC3A2 (also known as CD98), a subunit of the major leucine transporter,
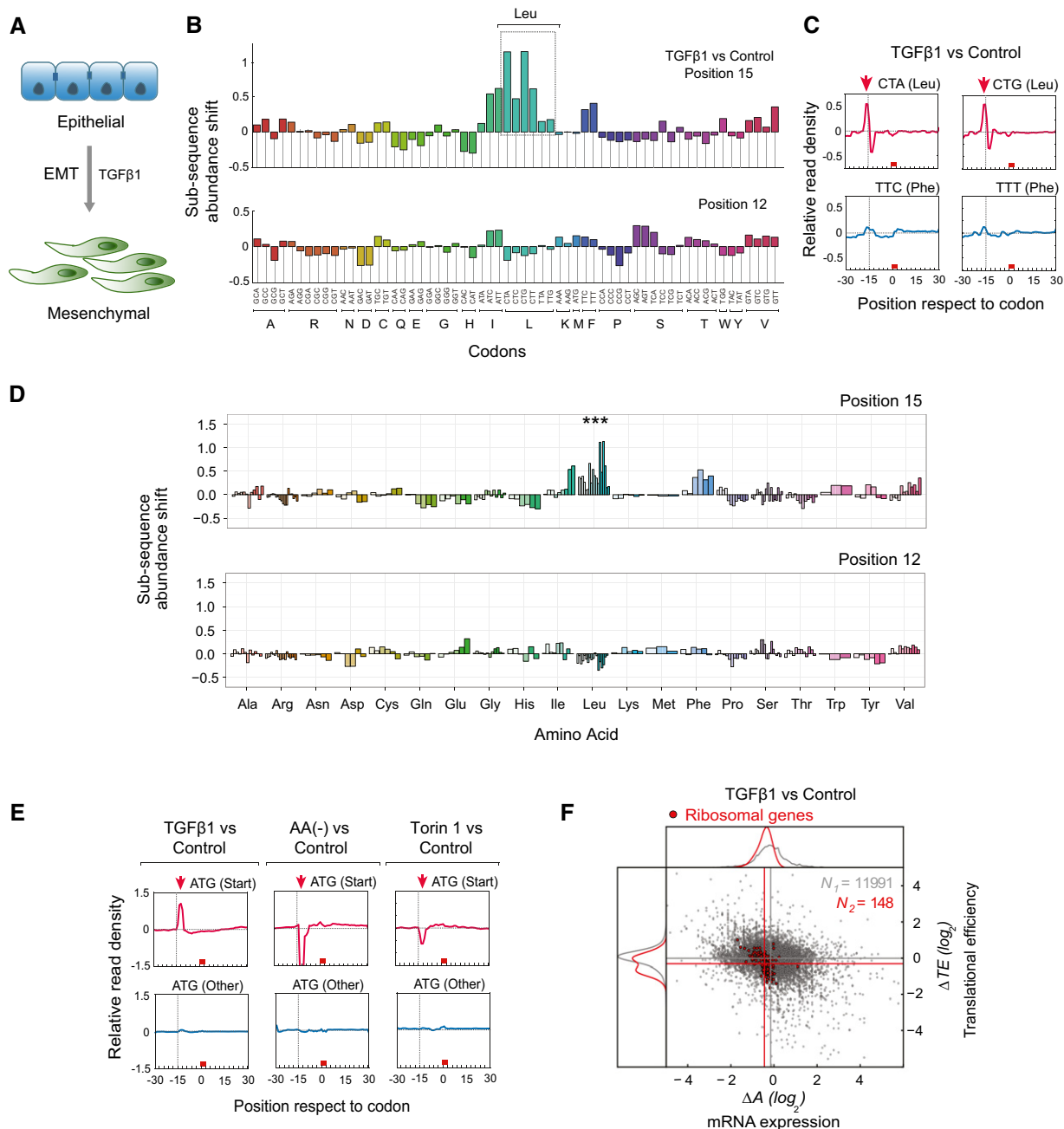
Figure 1. *Diricore* detects signal at leucine codons in cells treated with TGFβ1.

A   MCF-10A cells were treated with TGFβ1 (10 ng/ml) for 48 h.

B, C   *Diricore* analysis of MCF-10A cells treated with TGFβ1. The panels in (B) show subsequence analysis and the (C) panels 5′ RPF density analyses. The RPF density analysis shows increased signal of leucine at position 15 and decreased at position 12 (see Materials and Methods section).

D   Subsequence shift data from three biological replicates of *Diricore* analysis in MCF10A cells treated with TGFβ1 for 48 h, in which significant shifts at the amino acid level are displayed. Subsequence shifts are calculated by counting codon occurrences in RPFs, normalized within and averaged over genes, with respect to untreated controls. A mixed linear model, in which amino acids are fixed effects and codons are random effects, is used to test for deviating shifts at the amino acid level (*** FDR ≤ 0.001).

E   5′ RPF density analysis of the initiator ATG (START) of MCF-10A cells treated either with TGFβ1 for 48 h, or amino acid depletion or mTOR inhibition by Torin-1 for 2 h.

F   Changes in translational efficiencies of ribosomal proteins in response to TGFβ1 treatment.

was down ~twofold. We used snail2 (SNAI2), a key TGFβ1 target, and beta-actin (ActB) as positive and negative controls, respectively. Using flow cytometry analysis and qRT–PCR, we validated SLC3A2 downregulation following TGFβ1 treatment (Fig 2F). Downregulation of SLC3A2 transcript was observed also in additional TGFβ1-responsive cell lines (Fig EV5A), indicating that this effect is not
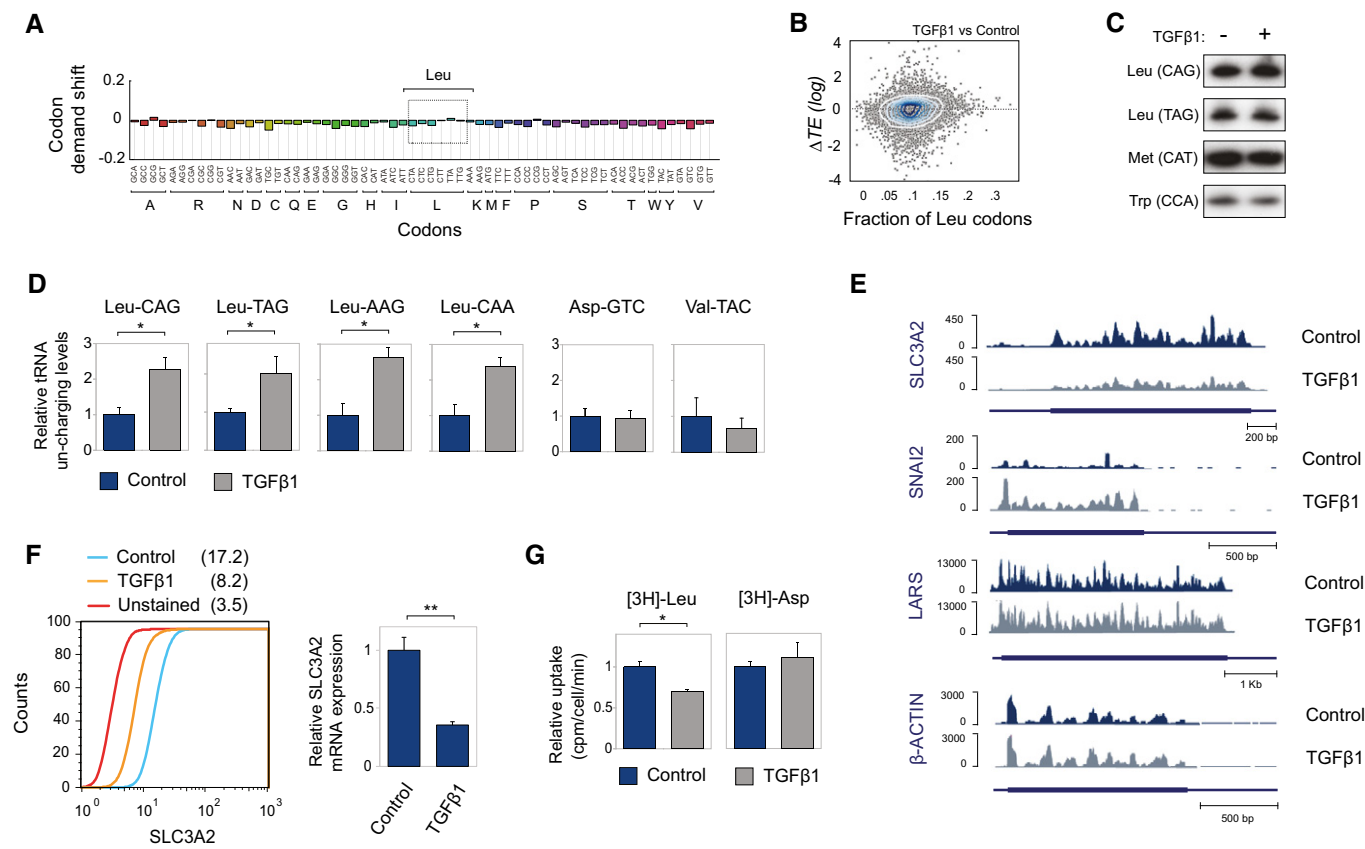
Figure 2. *Diricore* links regulation of leucine transporter levels to TGFβ1 signalling.

A   mRNA expression analysis for codon demand, based on the data from Fig 1A. The leucine codons are indicated (see Materials and Methods section).

B   Analysis of translational efficiency changes (ΔTE) versus leucine codon content of genes.

C   MCF-10A cells were treated with TGFβ1 for 48 h, and subjected to a northern blot analysis for the indicated tRNAs.

D   MCF-10A cells were treated as in panel (C), and subjected to tRNA aminoacylation analysis [17] for the indicated tRNAs. Error bars represent SD; *n* = 3; *P < 0.05 by Student's *t*-test.

E   Ribo-seq-based expression analysis of the indicated genes shows suppression of SLC3A2, an essential component of the leucine transporter in the cell.

F   MCF-10A cells, treated or not with TGFβ1 for 48 h, were subjected to flow cytometric analysis with anti-SLC3A2 antibody (left panel) and to qRT–PCR analysis for SLC3A2 (right panel). Error bars represent SD; *n* = 3; **P < 0.01 by Student's *t*-test.

G   The uptake of [3H]-Leu and control [3H]-Asp was measured in MCF-10A cells that were treated as in panel A. Error bars represent SD; *n* = 3; *P < 0.05 by Student's *t*-test.

restricted to MCF-10A cells. A time course experiment showed a rapid downregulation of SLC3A2 mRNA in response to TGFβ1 stimulation, suggesting mainly transcriptional control (Fig EV5B). Last, if the leucine amino acid transporter is involved in generating the leucine-*diricore* signal, reduced cellular uptake of leucine is predicted. Indeed, the uptake of leucine, but not control aspartic acid, was reduced in MCF10A treated with TGFβ1 (Fig 2G). Thus, reduced SLC3A2 leucine-transporter level coincides with the increase in *diricore* signal at leucine codons following TGFβ1 treatment.

Next, we postulated that if TGFβ1 limits uptake of leucine, artificial increase in cellular leucine availability should weaken the *diricore* signal in a specific manner. To examine this assumption, we reduced restraints in leucine transportation by adding to the medium esterified-leucine (eLeucine, a leucine analogue that can move across membranes and be used for protein synthesis, [22]). We induced MCF-10A cells with TGFβ1 for 48 h in the presence of eLeucine or control vehicle and first tested Leu-tRNA

aminoacylation. Figure 3A shows the expected increase in uncharged Leu-tRNA following TGFβ1 and reveals a significant attenuation of this effect by eLeucine. We use Val-tRNA aminoacylation as control, and this remained unaffected. Then, we used the same cell populations, profiled ribosomes and examined RPFs by *diricore*. Figure 3B and C show that while mock-treated cells elicited the expected leucine-*diricore* signal at position 15, the addition of eLeucine abrogated this signal in a specific manner. Furthermore, we controlled global cellular response to TGFβ1 by examining SNAI2 expression levels. This indicated comparable changes in both eLeucine and control conditions (Fig 3D). One of the most well-characterized cellular responses to TGFβ1 is cell growth arrest [23]. As expected, treatment with TGFβ1 reduced cell growth in MCF-10A cells. Intriguingly, eLeucine could partially rescue that phenotype (Fig 3E). These results strongly support the notion that TGFβ1 treatment affects leucine uptake in MCF10A cells and that this has consequences to TGFβ1-induced cell cycle control.
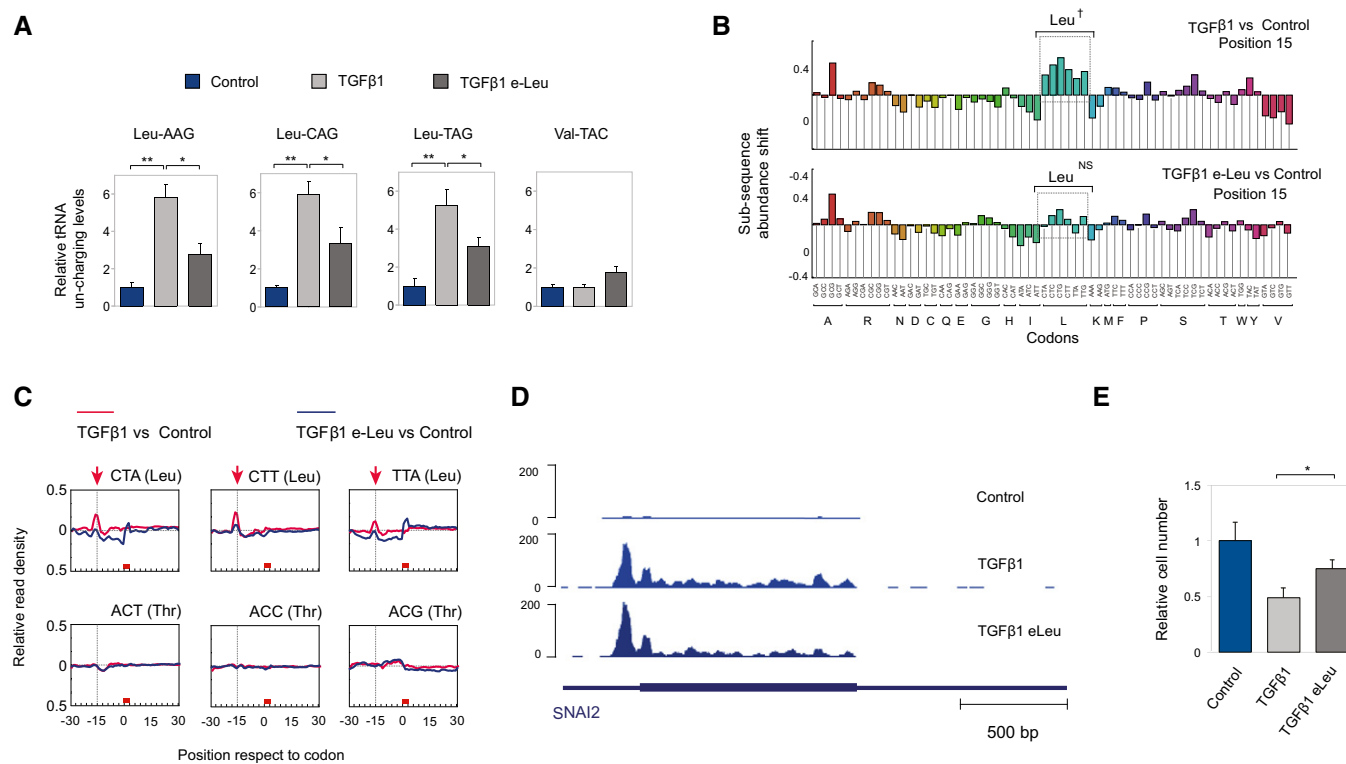
Figure 3. Addition of a membrane-permeable leucine analogue attenuates TGFβ1-induced *diricore* signals of leucine codons.

A   tRNA aminoacylation was performed with MCF10A cells treated with TGFβ1, complemented with either esterified-leucine (e-Leu) or control vehicle. Error bars represent SD; $n = 3$; **$P < 0.01$; *$P < 0.05$ by Student's *t*-test.

B, C *diricore* analysis of the same cell populations as described in panel (A). Panel (B) shows subsequence analysis of the data, and panel (C) RPF density analysis. In both cases, specific leucine signals at position 15 were markedly attenuated by the addition of eLeucine. [†]$P = 1.28e-04$ for CTG, $P = 1.22e-03$ for CTC, $P = 3.66e-03$ for CTT, $P = 1.23e-02$ for CTA, $P = 9.61e-03$ for TTG, and $P = 5.07e-02$ for TTA Leu codons by out of frame analysis. NS, no significance for any of the Leu codons by out of frame analysis.

D   Ribo-Seq-based expression analysis of SNAI2.

E   MCF-10A cells were treated as in (A), Cells were counted 24 h after treatment to assess proliferation. Error bars represent SD; $n = 3$; *$P < 0.05$ by Student's *t*-test.

Next, we asked whether SLC3A2 is causal to the *diricore* signals following TGFβ1 treatment using knockdown and overexpression tools. We first knocked down SLC3A2 by RNAi and confirmed suppression of expression and functionality by qRT–PCR, flow cytometry and reduced uptake rate of leucine (Fig 4A–C). As expected, knockdown of SLC3A2 resulted in a mild reduction in the phosphorylation of S6K and 4EBP1 (Fig EV6B). Furthermore, tRNA aminoacylation assays showed a significant increase in uncharged Leu-tRNAs, but not in control Asp- and arginine (Arg)-tRNAs, following SLC3A2 knockdown, suggesting a specific effect of SLCA2 on Leu-tRNAs (Fig 4D). Interestingly, *diricore* analysis identified a signal at leucine codons caused by SLC3A2 siRNAs, which was comparable to TGFβ1 in control siRNA-transfected cells (Figs 4E and EV6A). In contrast, the major TGFβ1 target, SNAI2, was not induced by SLC3A2 knockdown (Fig 4F), indicating that the leucine-*diricore* signal in the SLC3A2 siRNA-transfected cells was not due to aberrant activation of TGFβ1 signalling. Furthermore, SLC3A2 downregulation attenuated cell growth in a similar extent than TGFβ1 (Fig 4G). Thus, optimal expression level of SLC3A2 transporter in MCF-10A cells is important to maintain optimal levels of cellular leucine, Leu-tRNA charging and effective translation through leucine codons.

If SLC3A2 reduction limits availability of cellular leucine following TGFβ1 treatment, we postulated that high SLC3A2 levels would relieve this limitation, resulting in attenuation of leucine signal in *diricore*. To examine this issue, we overexpressed SLC3A2 in MCF-10A cells and treated them with TGFβ1. Figure 5A–D shows that overexpression of SLC3A2 stimulated leucine uptake, prevented the decrease in aminoacylation of Leu-tRNA following TGFβ1 treatment, and importantly attenuated the signal of *diricore* at leucine reading codons (Figs 5D and EV6B). The attenuation of the leucine effect by SLC3A2 overexpression was despite full activation of the TGFβ1 response (Fig 5E). Furthermore, SLC3A2 upregulation attenuated the TGFβ1-induced cell growth arrest (Fig 5F). Taken together, using *diricore* we uncovered a causal key role of SLC3A2 in limiting intracellular levels of leucine following TGFβ1 treatment.

To test the impact of SLC3A2 overexpression on EMT, we analysed the translational response of genes involved in this process. Expression of SLC3A2 did not affect the expression of genes involved in EMT (Fig EV6D). On the contrary, expression of SLC3A2 rescued the translational inhibition of ribosomal proteins induced by TGFβ1 (Fig EV6D). Our data indicate that while the overexpression of SLC3A2 rescues the uptake of leucine and the stalling of
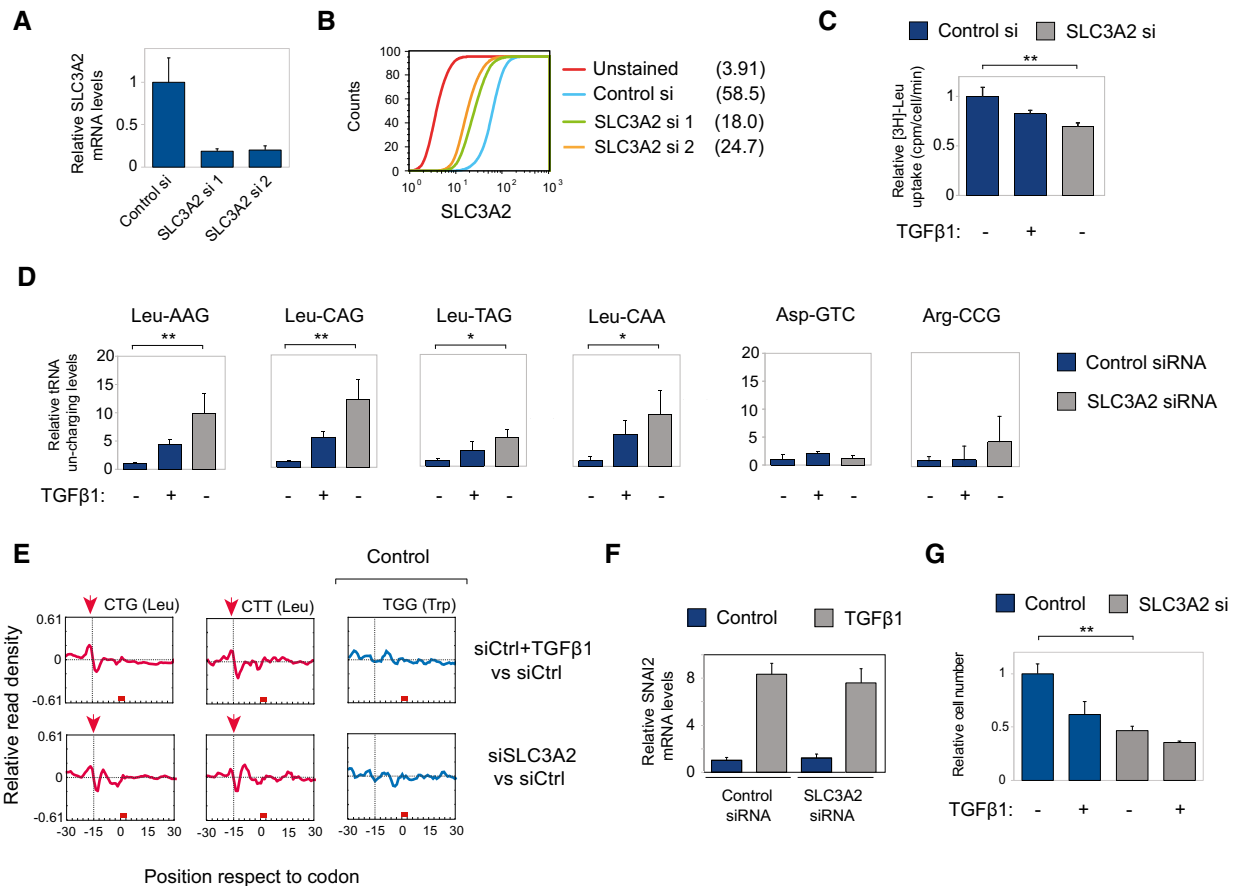
Figure 4. SLC3A2 downregulation in MCF-10A cells elicits *diricore* signals at leucine codons.

A MCF10A cells were transfected with siRNAs against SLC3A2 and control, and subjected to qRT–PCR analysis. Error bars represent SD; *n* = 3.

B MCF-10A cells treated as in (A) were subjected to flow cytometry analysis with anti-SLC3A2 antibody.

C The uptake of [3H]-Leu was measured in MCF10A cells transfected with SLC3A2 and control siRNAs treated or not with TGFβ1. Error bars represent SD; *n* = 3; **P < 0.01 by Student's *t*-test.

D MCF10A were treated as in panel (B) and subjected to tRNA aminoacylation analysis for the indicated tRNAs. Error bars represent SD; *n* = 3; **P < 0.01; *P < 0.05 by Student's *t*-test.

E *Diricore* analysis of MCF10A cells treated as in panel (B).

F The relative levels of SNAI2 mRNA, a major target of TGFβ1 signalling, were determined by qRT–PCR in cells treated as in panel (B). Error bars represent SD; *n* = 3.

G MCF10A cells transfected with SLC3A2 siRNA were treated with TGFβ1 for 48 h, and cells were counted to assess proliferation. Error bars represent SD; *n* = 3; **P < 0.01 by Student's *t*-test.

ribosomes, it does not affect EMT but it regulates the expression of genes involved in protein synthesis.

We used ribosome profiling (Ribo-seq) to study changes in amino acid availability in a cellular model that rapidly responds to TGFβ1. This is an important pathway involved in acquired resistance of tumour cells to chemotherapy, and uncovering such changes may assist in developing novel strategies to overcome chemoresistance. Previous studies have found that the translational regulatory layer is important for the TGFβ1 response [24,25]. Though amino acid shortages can be elicited by a multitude of effects, in proliferating cells mRNA translation and ribosome progression can be used to indicate amino acid deficiencies. We recently demonstrated that *diricore* (differential ribosome codon reading), a Ribo-seq-based method, can uncover amino acid deficiencies in tumours by comparing global ribosome positions between any test biological state and its control [17]. In certain

types of tumours, we identified proline shortage that represents a vulnerability in cancer. Here, we show that following TGFβ1 treatment mild shortage in leucine availability is formed due to a reduction in the level of its transporter (Fig 5F). In the context of mesenchymal cells, reduced level of leucine uptake triggers a mild inhibition of mTOR and reduced the ribosome occupancy of mTOR target genes. Reduced leucine uptake rate may serve to balance proliferation and metabolic changes activated by TGFβ1 to induce EMT.

Ribo-seq has been extensively used to explore protein translation programs at a genomic scale. Beyond this application, we have recently demonstrated that Ribo-seq can measure mitochondrial translation and unravel mechanisms of action of disease-triggering mitochondria mutations [26]. Differential examination of ribosome occupancy of normal and patient-derived mitochondria by Ribo-seq can pinpoint causal disease pathways without *a priori* genetic
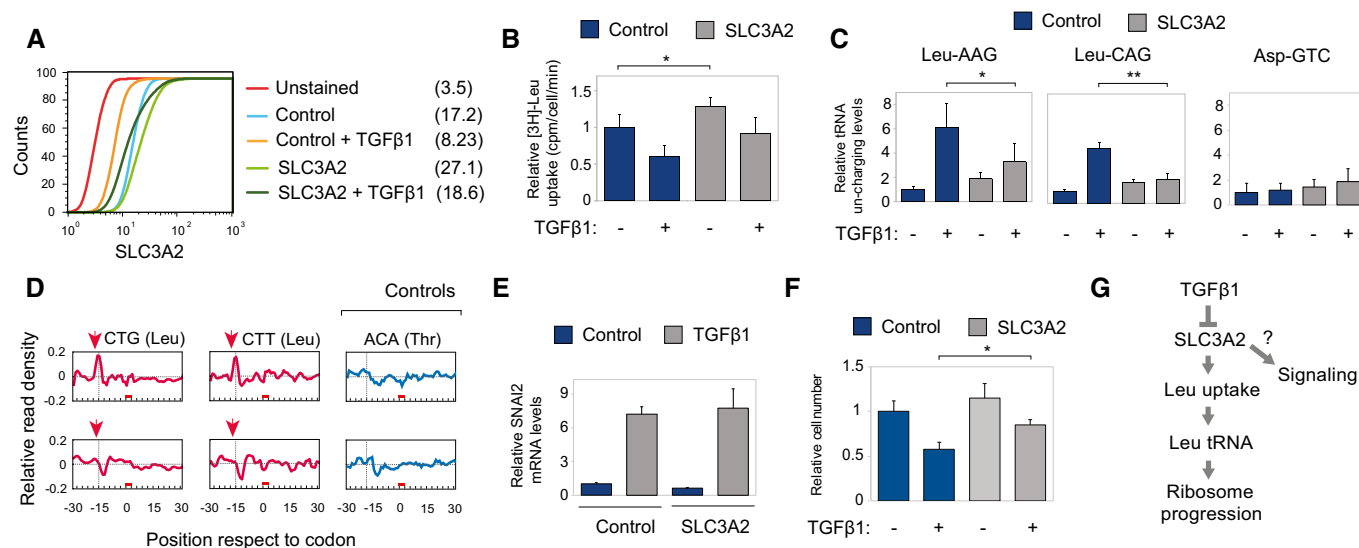
Figure 5. Upregulation of SLC3A2 relieves leucine shortage induced by TGFβ1.

A   Flow cytometry analysis with anti-SLC3A2 antibody of stable control and SLC3A2-overexpressing (marked SLC3A2) polyclonal MCF10A populations.

B   [^{3}H]- Leu uptake analysis of MCF10A populations as marked, treated or not with TGFβ1 for 48 h. Error bars represent SD; n = 3; *P < 0.05 by Student's t-test.

C   The same cell populations as in panel (B) were subjected to tRNA aminoacylation analysis for the indicated tRNAs. Error bars represent SD; n = 3; **P < 0.01; *P < 0.05 by Student's t-test.

D   *Diricore* analysis of leucine and control threonine codons in the same cell populations as presented in panel (B).

E   The relative induction level of SNAI2 mRNA was measured in the same cell populations as in panel (B). Error bars represent SD; n = 3.

F   Control and SLC3A2 overexpressing cells were treated with TGFβ1 for 48 h and cells were counted to assess proliferation. Error bars represent SD; n = 3; *P < 0.05 by Student's t-test.

G   Schematic summary of our findings.

knowledge. In a similar way, Ishimura R *et al* have recently unmasked the disease potential of mutations in nuclear-encoded tRNA genes [27]. Last, we expanded the Ribo-seq utilities even further and used it as a cellular biological sensor mechanism for amino acid deficiencies [17].

Following TGFβ1 treatment and induction of EMT, *diricore* has identified shortage in leucine. At least part of this effect can be explained by the reduced expression of the leucine transporter SLC3A2 (which together with SLC7A5 forms the large neutral amino acid transporter LAT1 in cells) triggering reduced uptake levels of the amino acid leucine. We found that SLC3A2 downregulation is TGFβ1-dependent. The mechanism of SLC3A2 inhibition remains yet to be resolved. However, SLC3A2 is found upregulated in a wide variety of cancers and its expression correlates with poor prognosis [28]. How exactly SLC3A2 contributes to tumorigenesis is unclear, and whether the regulation of leucine uptake following TGFβ1 bares functional consequences to the EMT process and cancer remains to be explored. SLC3A2 has been linked to integrin signalling [29] and it was shown that the transcriptional co-activators YAP and TAZ (YAP/TAZ) activate the leucine transporter to increase leucine uptake and modulate mTOR signalling [30]. TGFβ1 was already connected to YAP/TAZ signalling, suggesting that in our cellular system too YAP/DAZ controls leucine uptake following EMT. Nevertheless, the elucidation of the causal events leading to reduced leucine uptake following TGFβ1 treatment validates the finding of leucine deficiencies by *diricore*, and opens up novel avenues in challenging the phenomenon of EMT-associated chemoresistant tumours.

Materials and Methods

Cell culture

MCF10A and MCF10A-inducible RAS[V12] cells were cultured in DMEM/F12 1:1 medium supplemented with 5% horse serum, EGF (10 ng/ml), insulin (10 μg/ml), cholera toxin (100 ng/ml) and hydrocortisone (500 ng/ml) in 5% CO_2 at 37°C. Small interfering RNAs (siRNAs) against *SLC3A2* were purchased from Life Technologies (Grand Island, NY, USA). MCF10a cells were transfected using Dharmafect I reagent (Dharmacon) following the manufacturer's instructions. For TGFβ1 treatment, MCF10a cells were treated with human recombinant TGFβ1 (10 ng/ml) for 48 h (R&D Systems).

Ribosome profiling (Ribo-Seq)

Libraries from cultured cells were prepared as described previously [26]. Lysates were centrifuged at 2,655 g, and the supernatant was digested with 2 U/μl of RNase I (Life Technologies, Grand Island, NY, USA) for 45 min at room temperature. Resulting monosomes were purified, RNA was isolated, and RP libraries were prepared as described previously.

RNA sequencing

Total RNA was isolated using TRIzol Reagent (Invitrogen), following the manufacturer's instructions. Poly(A) was isolated using the Oligotex mRNA mini kit (Qiagen). Libraries were prepared using the

TruSeq RNA sample preparation kit (Illumina) following the manufacturer's instructions.

Leucine and aspartic acid uptake

Cells were plated in 12-well plates (1×10^5 cells/well). When the cells reached 80% confluence, they were washed twice in PBS and incubated for 5 min either in sodium-free uptake buffer (4.8 mM KCl, 1.3 mM $CaCl_2$, 1.2 mM $MgSO_4$, 25 mM HEPES, 1.2 mM KH2PO4, 5.6 mM glucose, pH 7.4) for Leu or in PBS for Asp. Cells were incubated for 5 min with either [3H] L-leucine or [3H] L-aspartic acid. Uptake was finished by washing the cells three times with ice-cold uptake solution or PBS. Cells were solubilized in 0.1 N NaOH, and radioactivity was counted by liquid scintillation.

Northern blot

4 μg of total RNA was separated on a 10% denaturing polyacrylamide gel and transferred onto a nylon membrane (Hybond-N+; Amersham Biosciences). The membrane was UV-crosslinked, dried and hybridized using radiolabelled RNA probes in NorthernMax buffer (Ambion). Riboprobes were synthesized using the miRNA probe construction kit (Ambion) following the manufacturer's instructions.

Real-time PCR

1 μg of total RNA was reverse transcribed using the SuperScript III first-strand synthesis system (Life Technologies) following the manufacturer's instructions. Real-time PCR was performed using the SensiFAST SYBR real-time PCR kit (Bioline).

Metabolite profiling

MCF10A cells were seeded in triplicate wells of 6-well plates at a density of 5×10^5 cells per well. After 24 h, media was replaced and cells were harvested after 48 h. Cells were washed with ice-cold PBS and metabolites were extracted in 1 ml lysis buffer containing methanol/acetonitrile/dH$_2$O (2:2:1). Samples were spun at 16,000 *g* for 15 min at 4°C, and supernatants were collected for LC-MS analysis. LC-MS analysis was performed on an Exactive mass spectrometer (Thermo Scientific) coupled with a Dionex Ultimate 3000 autosampler and pump (Thermo Scientific). The MS operated in polarity-switching mode with spray voltages of 4.5 kV and −3.5 kV. Metabolites were separated using a Sequant ZIC-pHILIC column (2.1 × 150 mm, 5 μm, guard column 2.1 × 20 mm, 5 μm; Merck) with elution buffers acetonitrile and eluent A (20 mM (NH_4)$_2CO_3$, 0.1% NH_4OH in ULC/MS grade water (Biosolve)). Flow rate was set at 150 μl/min and gradient ran from 20% A to 60% A in 20 min, followed by a wash at 80% A and re-equilibration at 20% A. Metabolites were identified and quantified using LCquan software (Thermo Scientific) on the basis of exact mass within 5 ppm and further validated by concordance with retention times of standards. Metabolites were quantified using LCquan software (Thermo Scientific). Peak intensities were normalized based on median peak intensity.

Diricore analysis

Preprocessing and alignment of the sequencing data was described earlier. Subsequence analysis, RPF density analysis and codon demand analysis was performed as described earlier (Loayza-Puch, 2016).

Expanded View for this article is available online.

Author contributions

FL-P, KR and RA designed the experimental strategy of all the experiments and wrote the manuscript. FL-P and JZ conducted ribosome profiling experiments and most of the biochemical experiments on the study. KR performed all the bioinformatics and statistical analysis. JFOV prepared overexpression constructs and established cell line models. RL performed the FACS experiments. APU prepared RNA-seq libraries. EAZ and CRB performed metabolite profiling. BM performed gene expression analysis.

Conflict of interest

The authors declare that they have no conflict of interest.

References

1. Shi Y, Massague J (2003) Mechanisms of TGF-beta signaling from cell membrane to the nucleus. *Cell* 113: 685−700
2. Massague J, Gomis RR (2006) The logic of TGFbeta signaling. *FEBS Lett* 580: 2811−2820
3. Massague J (2012) TGFbeta signalling in context. *Nat Rev Mol Cell Biol* 13: 616−630
4. Frederick JP, Liberati NT, Waddell DS, Shi Y, Wang XF (2004) Transforming growth factor beta-mediated transcriptional repression of c-myc is dependent on direct binding of Smad3 to a novel repressive Smad binding element. *Mol Cell Biol* 24: 2546−2559
5. Polyak K, Kato JY, Solomon MJ, Sherr CJ, Massague J, Roberts JM, Koff A (1994) p27Kip1, a cyclin-Cdk inhibitor, links transforming growth factor-beta and contact inhibition to cell cycle arrest. *Genes Dev* 8: 9−22
6. Laiho M, Weis MB, Massague J (1990) Concomitant loss of transforming growth factor (TGF)-beta receptor types I and II in TGF-beta-resistant cell mutants implicates both receptor types in signal transduction. *J Biol Chem* 265: 18518−18524
7. Siegel PM, Massague J (2003) Cytostatic and apoptotic actions of TGF-beta in homeostasis and cancer. *Nat Rev Cancer* 3: 807−821
8. Ansieau S, Bastid J, Doreau A, Morel AP, Bouchet BP, Thomas C, Fauvet F, Puisieux I, Doglioni C, Piccinin S *et al* (2008) Induction of EMT by twist proteins as a collateral effect of tumor-promoting inactivation of premature senescence. *Cancer Cell* 14: 79−89

9. Kalluri R, Weinberg RA (2009) The basics of epithelial-mesenchymal transition. *J Clin Invest* 119: 1420 – 1428

10. Thiery JP, Acloque H, Huang RY, Nieto MA (2009) Epithelial-mesench-ymal transitions in development and disease. *Cell* 139: 871 – 890

11. Jiang L, Xiao L, Sugiura H, Huang X, Ali A, Kuro-o M, Deberardinis RJ, Boothman DA (2015) Metabolic reprogramming during TGFbeta1-induced epithelial-to-mesenchymal transition. *Oncogene* 34: 3908 – 3916

12. Guido C, Whitaker-Menezes D, Capparelli C, Balliet R, Lin Z, Pestell RG, Howell A, Aquila S, Ando S, Martinez-Outschoorn U *et al* (2012) Meta-bolic reprogramming of cancer-associated fibroblasts by TGF-beta drives tumor growth: connecting TGF-beta signaling with "Warburg-like" cancer metabolism and L-lactate production. *Cell Cycle* 11: 3019 – 3035

13. Shaul YD, Freinkman E, Comb WC, Cantor JR, Tam WL, Thiru P, Kim D, Kanarek N, Pacold ME, Chen WW *et al* (2014) Dihydropyrimidine accu-mulation is required for the epithelial-mesenchymal transition. *Cell* 158: 1094 – 1109

14. Dong C, Yuan T, Wu Y, Wang Y, Fan TW, Miriyala S, Lin Y, Yao J, Shi J, Kang T *et al* (2013) Loss of FBP1 by Snail-mediated repression provides metabolic advantages in basal-like breast cancer. *Cancer Cell* 23: 316 – 331

15. LeBleu VS, O'Connell JT, Gonzalez Herrera KN, Wikman H, Pantel K, Haigis MC, de Carvalho FM, Damascena A, Domingos Chinen LT, Rocha RM *et al* (2014) PGC-1alpha mediates mitochondrial biogenesis and oxidative phosphorylation in cancer cells to promote metastasis. *Nat Cell Biol* 16: 992 – 1003, 1-15

16. Bassik MC, Lebbink RJ, Churchman LS, Ingolia NT, Patena W, LeProust EM, Schuldiner M, Weissman JS, McManus MT (2009) Rapid creation and quantitative monitoring of high coverage shRNA libraries. *Nat Methods* 6: 443 – 445

17. Loayza-Puch F, Rooijers K, Buil LC, Zijlstra J, Oude Vrielink JF, Lopes R, Ugalde AP, van Breugel P, Hofland I, Wesseling J *et al* (2016) Tumour-specific proline vulnerability uncovered by differential ribosome codon reading. *Nature* 530: 490 – 494

18. De Craene B, Berx G (2013) Regulatory networks defining EMT during cancer initiation and progression. *Nat Rev Cancer* 13: 97 – 110

19. Lamouille S, Xu J, Derynck R (2014) Molecular mechanisms of epithelial-mesenchymal transition. *Nat Rev Mol Cell Biol* 15: 178 – 196

20. Saxton RA, Knockenhauer KE, Wolfson RL, Chantranupong L, Pacold ME, Wang T, Schwartz TU, Sabatini DM (2016) Structural basis

21. for leucine sensing by the Sestrin2-mTORC1 pathway. *Science* 351: 53 – 58

22. Efeyan A, Sabatini DM (2013) Nutrients and growth factors in mTORC1 activation. *Biochem Soc Trans* 41: 902 – 905

23. Thiele DL, Lipsky PE (1990) The action of leucyl-leucine methyl ester on cytotoxic lymphocytes requires uptake by a novel dipeptide-specific facilitated transport system and dipeptidyl peptidase I-mediated conver-sion to membranolytic products. *J Exp Med* 172: 183 – 194

24. Rahimi RA, Leof EB (2007) TGF-beta signaling: a tale of two responses. *J Cell Biochem* 102: 593 – 608

25. Waerner T, Alacakaptan M, Tamir I, Oberauer R, Gal A, Brabletz T, Schreiber M, Jechlinger M, Beug H (2006) ILEI: a cytokine essential for EMT, tumor formation, and late events in metastasis in epithelial cells. *Cancer Cell* 10: 227 – 239

26. Hussey GS, Link LA, Brown AS, Howley BV, Chaudhury A, Howe PH (2012) Establishment of a TGFbeta-induced post-transcriptional EMT gene signature. *PLoS ONE* 7: e52624

27. Loayza-Puch F, Drost J, Rooijers K, Lopes R, Elkon R, Agami R (2013) p53 induces transcriptional and translational programs to suppress cell proliferation and growth. *Genome Biol* 14: R32

28. Ishimura R, Nagy G, Dotu I, Zhou H, Yang XL, Schimmel P, Senju S, Nishimura Y, Chuang JH, Ackerman SL (2014) RNA function. Ribosome stalling induced by mutation of a CNS-specific tRNA causes neurode-generation. *Science* 345: 455 – 459

29. Fei F, Li X, Xu L, Li D, Zhang Z, Guo X, Yang H, Chen Z, Xing J (2014) CD147-CD98hc complex contributes to poor prognosis of non-small cell lung cancer patients through promoting cell proliferation via the PI3K/Akt signaling pathway. *Ann Surg Oncol* 21: 4359 – 4368

30. Poettler M, Unseld M, Braemswig K, Haitel A, Zielinski CC, Prager GW (2013) CD98hc (SLC3A2) drives integrin-dependent renal cancer cell behavior. *Mol Cancer* 12: 169

31. Hansen CG, Ng YL, Lam WL, Plouffe SW, Guan KL (2015) The Hippo pathway effectors YAP and TAZ promote cell growth by modulating amino acid signaling to mTORC1. *Cell Res* 25: 1299 – 1313

32. Subramanian A, Tamayo P, Mootha VK, Mukherjee S, Ebert BL, Gillette MA, Paulovich A, Pomeroy SL, Golub TR, Lander ES *et al* (2005) Gene set enrichment analysis: a knowledge-based approach for interpreting genome-wide expression profiles. *Proc Natl Acad Sci USA* 102: 15545 – 15550